TRANSMISSION ELECTRON MICROSCOPIC STUDY OF DIAGENETIC CHLORITE IN GULF COAST ARGILLACEOUS SEDIMENTS[1]

JUNG HO AHN AND DONALD R. PEACOR

Department of Geological Sciences, The University of Michigan
Ann Arbor, Michigan 48109

Abstract—Transmission and analytical electron microscopy have been used to study the diagenesis of the trioctahedral component of phyllosilicates (principally chlorite) in argillaceous core samples (depths of 1750, 2450, and 5500 m) from the Gulf Coast. Chlorite was observed as 100–150-Å thick packets intergrown within mixed-layer illite/smectite in the 2450-m sample and was more abundant and larger in packet thickness in the 5500-m sample. The chlorite is disordered in stacking sequence as characterized by diffuseness of reflections with $k \neq 3n$ in electron diffraction patterns. Berthierine (7-Å) was locally found to be intercalated within chlorite layers. Chlorite from the 5500-m sample is iron-rich and has an average chemical formula of $Fe_{3.1}Mg_{1.1}Al_{2.7}Si_{2.8}O_{10}(OH)_8$. This chemical composition and textural relations suggest that the chlorite formed within mixed-layer illite/smectite utilizing Fe and Mg released from the smectite during its conversion to illite. The berthierine is nearly identical in chemical composition with the coexisting chlorite although it may have a slightly higher Fe content. The 7-Å berthierine is probably a metastable precursor of the chlorite and may be diagnostic of the diagenetic environment.

Key Words—Berthierine, Chlorite, Diagenesis, Illite/smectite, Transmission electron microscopy.

INTRODUCTION

Chlorite is one of the most abundant phyllosilicates and is most frequently encountered in sedimentary and low-grade metamorphic rocks. It increases in abundance along with illite with increasing depth in argillaceous sediments (Dunoyer de Segonzac, 1970; Muffler and White, 1969; Weaver and Beck, 1971; Hower *et al.*, 1976; Boles and Franks, 1979). Such changes in proportions of phyllosilicates with depth are generally attributed to burial diagenetic reactions in argillaceous sediments, but the specific process of chlorite formation during burial diagenesis is still unclear.

Hower *et al.* (1976) investigated diagenetic changes in clay minerals in argillaceous sediments using Gulf Coast core samples. Their mineralogical and chemical evidence of burial diagenetic change was based largely on X-ray powder diffraction (XRD) studies and bulk chemical analyses of the clay-size fractions. They observed that mixed-layer illite/smectite (I/S) underwent conversion from >20% to ≃80% illite layers over the depth interval 2000–3700 m. Chlorite was first detected at a depth of 2500 m and increased in abundance down to 3700 m, below which it remained almost constant in abundance. These authors concluded that all of the mineralogical changes were due to diagenetic reactions rather than to primary chemical or miner-

alogical variations in the original sediments. They also suggested that the overall major reaction in the shale during diagenesis was smectite + K-feldspar + mica = illite + chlorite + quartz, and considered that the shale behaved as a closed system for all components except H_2O, CO_2, CaO, and Na_2O. Muffler and White (1969) described mineral distributions in the Salton Sea geothermal field as a function of temperature, and first found chlorite at 120°–220°C, a temperature range which is much higher than that of the Gulf Coast environment (70°C, as determined by Hower *et al.*, 1976).

It is generally considered that the diagenetic or authigenic chlorites from sedimentary rocks are iron-rich (Velde *et al.*, 1974; Velde, 1977), but relatively little is known about the chemical composition of chlorite found in argillaceous sediments affected by burial diagenesis. This lack of information exists in part because individual chlorite grains cannot be separated and cannot be analyzed by the electron microprobe due to their small grain size and mixed layering with other phyllosilicates. In addition, little is known about their textural relationships with other phases because the optical microscope and the scanning electron microscope (SEM) cannot reveal mixed-layering features or intergrowths of phyllosilicates, relations which are common in clay minerals from low-temperature environments (e.g., see Lee, 1984). In the present paper transmission electron microscopy (TEM) and analytical electron microscopy (AEM) have been used to determine detailed mineralogical, chemical, and structural relations and to document the changes that occur in chlorite during burial diagenesis.

228

SPECIMENS AND EXPERIMENTAL TECHNIQUE

Three specimens of shale cuttings from the 1750-, 2450-, and 5500-m depths of a well (Case Western Reserve University Gulf Coast 6) drilled in Oligocene–Miocene sediments of the Gulf Coast of the United States, were provided by John Hower. The mineralogy and chemistry of the specimens were described in detail by Hower *et al.* (1976) on the basis of XRD studies and chemical analyses of the clay-sized fractions as a function of burial depth. Hower *et al.* (1976) reported an increase in the illite content of I/S from 20% to 40% and finally to 80% with increasing depth. These observations were verified in the present investigation using an automated Philips XRG 3100 X-ray diffractometer preceding the TEM study.

Thin sections of cuttings were prepared perpendicular to the bedding plane to promote optimum orientation for lattice-fringe imaging of phyllosilicates in the TEM. Following optical examination, selected areas of the thin sections were detached, ion-thinned, and carbon coated. The ion-thinned samples were examined at 100 kV in a JEOL JEM-100CX scanning-transmission electron microscope (STEM) fitted with a solid state detector for energy dispersive analysis; the latter had X-ray spatial resolution approaching 300 Å. The modifications necessary for accurate quantitative analysis using this JEOL JEM-100CX instrument were discussed by Allard *et al.* (1980) and Blake *et al.* (1980). The specimens were tilted 45° to the incident electron beam, and raw X-ray data were collected over 100-sec counting times at 100×10^3 magnification for analysis. Thin edges (500–1000 Å) were analyzed quantitatively following the AEM procedures of Cliff and Lorimer (1975). This procedure minimized atomic number, absorption, and fluorescence effects. Proportionality constants ("k" values) for each element relative to Si were obtained by using ion-thinned clinochlore and fayalite as standard minerals at the same instrumental conditions and at the same magnification in the STEM mode as used for the ion-thinned shales. One-dimensional lattice fringe images were obtained in TEM observations by using only 00*l* diffractions as described by Iijima and Buseck (1978).

EXPERIMENTAL RESULTS

Diagenetic growth of chlorite with depth

No chlorite was observed in the 1750-m sample by the TEM examination, consistent with the XRD results of Hower *et al.* (1976). Minor chlorite was observed in the 2450-m samples as 100- to 150-Å thick packets intergrown with I/S. The chlorite was characterized on the basis of well-developed, straight 14-Å lattice fringes which represent each layer unit of chlorite structure, and from its electron diffraction patterns. In Figure 1 chlorite layers can be distinguished from I/S by their distinctly sharp, straight 14-Å lattice fringes which contrast with the wavy and discontinuous smectite-rich I/S which displays narrower 10-Å lattice fringes. Microstructural aspects of the I/S and the smectite-to-illite transformation were discussed by Ahn and Peacor (1984).

The chlorite packets within I/S are likely the incipient, earliest stage of chlorite formed during burial diagenesis, partly because no chlorite was observed from the shallower sample. More importantly, these chlorite layers were found to be intergrown with and semi-coherent with respect to the surrounding I/S. All layers constituted a continuous structural network of phyllosilicates. Figure 2 also shows packets of diagenetic chlorite in the 2450-m sample, which display interstratification of a packet of 10-Å layers and local 7-Å layers between 14-Å chlorite layers. Such 7-Å layers *interstratified within chlorite* are common throughout the 2450-m and 5500-m samples. Based on AEM data, the 7-Å layers are likely a trioctahedral phase, approximately berthierine in composition.

Chlorite is more abundant in the 5500-m sample, in accordance with previous XRD data (Hower *et al.*, 1976). The packets of chlorite layers are also much thicker than those in the 2450-m samples. The chlorite packets are subparallel to each other and are variable in packet thickness. High-magnification lattice fringe images of chlorite layers (Figure 3) from the 5500-m sample always showed local 7-Å layers; however, no apparent difference in the relative abundance of the 7-Å layers compared to those in the 2450-m sample was noted.

Polytypism of chlorite

Chlorite occurs as several distinct polytypes; mainly because alternating 2:1 layers (talc-like structure) and interlayer sheets (brucite-like structure) can have different relative positions and orientations. Most chlorites are either regular 1-layer structures or have a disordered structure characterized by sharp $k = 3n$ reflections and streaking of $k \neq 3n$ reflections. Brown and Bailey (1962) derived 12 ideal, regular 1-layer chlorite polytypes and suggested that the higher energy structures form metastably in low-energy environments and transform to a more stable structural arrangement with increasing temperature. Hayes (1970) found that the incipient diagenetic chlorite in sedimentary rocks is the poorly ordered metastable Ib_d polytype and suggested that this incipient chlorite is the first step in a sequence of crystallization or increasing stacking order from Ib_d to Ib ($\beta = 97°$) to Ib ($\beta = 90°$) with increasing temperature and depth, to the final, most stable polytype, IIb.

The chlorite grains from the 2450-m sample were too small to yield high-quality electron diffraction patterns; however those from the 5500-m samples were large enough to yield information on structure and
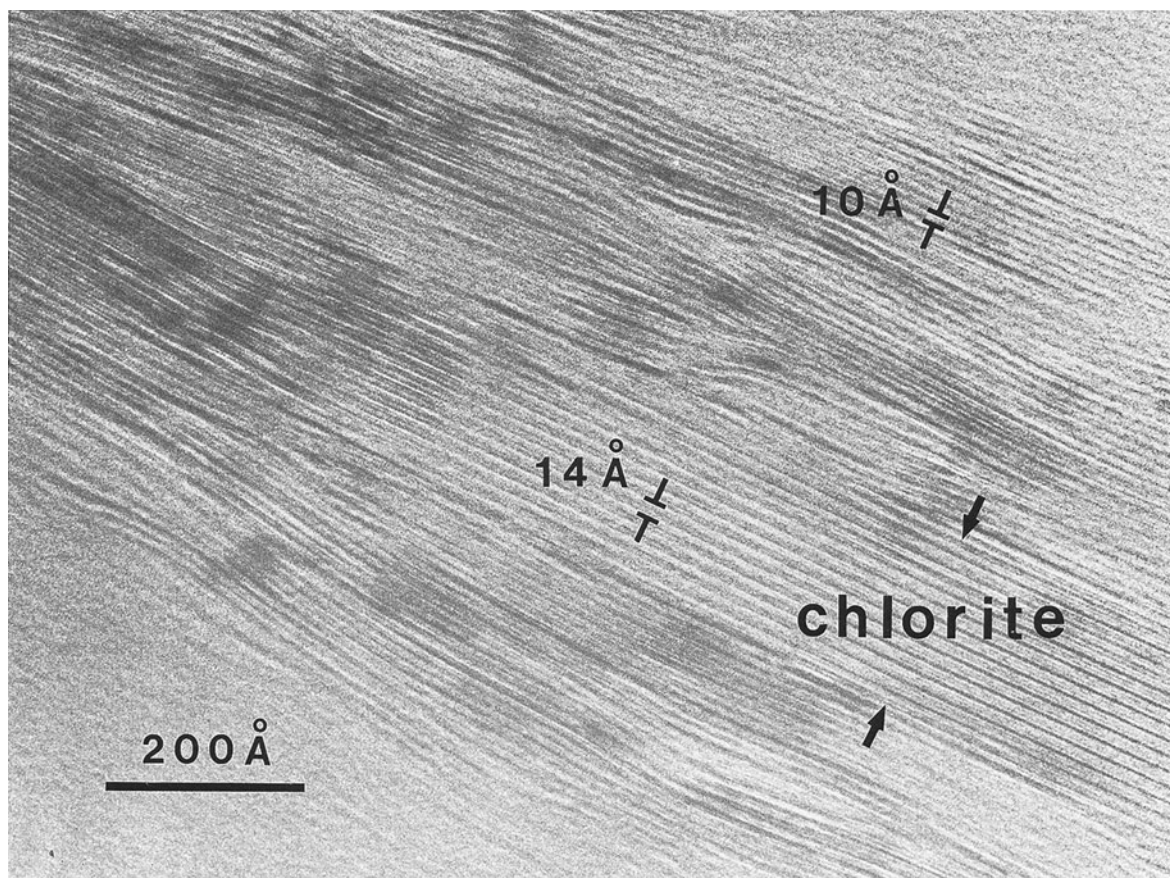
Figure 1. Lattice fringe image by transmission electron microscopy obtained from the 2450-m sample. A chlorite packet is intergrown with layers of mixed-layer illite/smectite.

stacking phenomena. With the incident electron beam oriented parallel to $[1\bar{1}0]$ or $[\bar{1}10]$, most of these chlorites exhibited electron diffraction patterns with heavy streaking along reciprocal lattice rows with $k \neq 3n$ and sharp reflections for rows with $k = 3n$ (Figure 4). Sharp reflections with $k = 3n$, but diffuse streaking for those with $k \neq 3n$ indicate that the talc-like layers and the brucite-like layers are related to one another by shifts of $\pm b/3$ along the three pseudohexagonal Y axes, although they are disordered as to relative position in adjacent 14-Å layer units (Brown and Bailey, 1962; Bailey, 1980). This kind of randomness in stacking sequence in chlorite has been termed semi-random stacking by Brown and Bailey (1962) who considered it to be common. The specific polytype could not be identified from the two-dimensional electron diffraction patterns in the present study, but it is inferred to be Ib$_d$, the dominant chlorite polytype in diagenetic environments (Brown and Bailey, 1962; Hayes, 1970).

Chemical composition of diagenetic chlorite

The chemical formulae of chlorites (Table 1) from the 5500-m sample were calculated on the anion basis of $O_{10}(OH)_8$ and on the assumption that 10% of total iron was Fe^{3+}, a reasonable average value for chlorite in diagenetic and low-grade metamorphic environments (McDowell and Elders, 1980). On this basis, the number of trivalent cations in the octahedral site was greater than the number of Al^{3+} in tetrahedral sites. This distribution caused an excess in positive charge which was compensated by assuming vacancies on the octahedral sites; the resultant formula, however, deviated from the ideal trioctahedral chlorite formula (Foster, 1962; Bailey, 1980; Brindley, 1982). The number of vacancies was equal to half of the excess R^{3+} in the octahedral sites. All analyses gave rise to formulae having 0.2 to 0.4 vacancies per 6 octahedral sites. Boles and Franks (1979) and McDowell and Elders (1980) also reported octahedral vacancies in chlorites based on electron microprobe data.

The chemical composition of chlorite from the Gulf Coast is typically iron-rich and would be called brunsvigite according to the chlorite classification scheme of Foster (1962). The AEM data show that the chemical composition of chlorite grains from the 5500-m sample does not vary significantly. A plot of compositions on
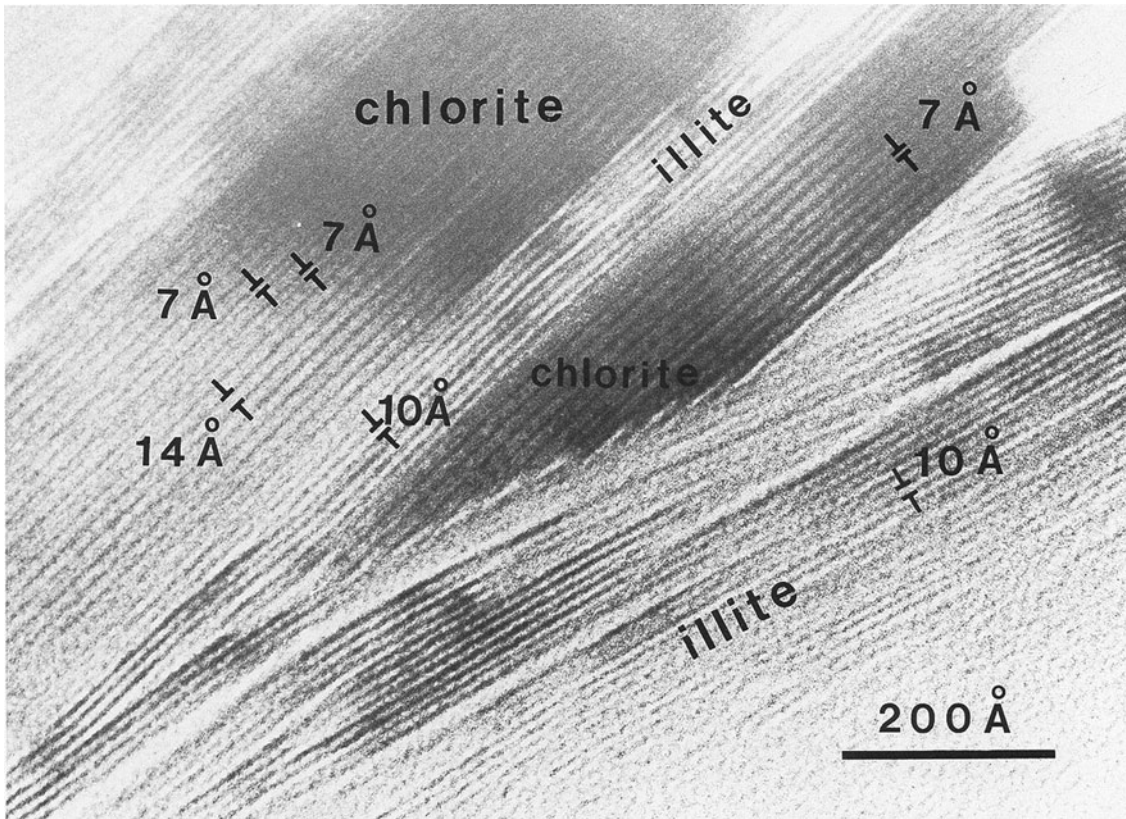
Figure 2.   Lattice fringe image by transmission electron microscopy obtained from the 2450-m sample showing packets of 10-Å illite layers interstratified with chlorite packets. Several 7-Å layers are interstratified with chlorite layers.

a Al-Fe-Mg diagram (Figure 5) shows that the diagenetic chlorite from the Gulf Coast is higher in Fe and Al than chlorites from higher-grade rocks.

Interstratification of 7-Å layers and chlorite layers

Although interstratification of chlorite and other 2:1 phyllosilicates is well known (e.g., April, 1981; Schreyer *et al.*, 1982; Maresch *et al.*, 1983; Veblen,
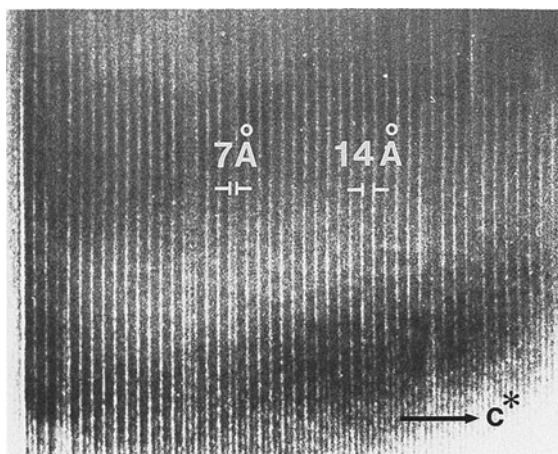

Figure 3.   High-magnification transmission electron microscopic image from the 5500-m sample showing chlorite lattice fringes. Locally, 7-Å layers are intercalated within 14-Å chlorite as 1- or 2-layer units.
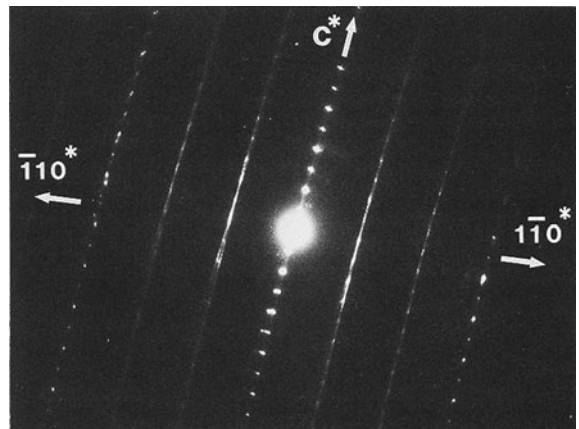

Figure 4.   Electron diffraction pattern of chlorite, showing streaking for reciprocal lattice rows with $k \neq 3n$. $1\bar{1}0^*$ and $\bar{1}10^*$ refer to the reciprocal lattice directions $[1\bar{1}0]$ and $[\bar{1}10]$.

Table 1. Analytical electron microscopic analyses of chlorite from the 5500-m sample.

Elements	[1]1	2	3	4	5	6	7	8	Average
Si	2.7	2.8	2.8	2.7	2.9	2.8	2.7	2.8	2.8
Al(IV)	1.3	1.2	1.2	1.3	1.1	1.2	1.3	1.2	1.2
Al(VI)	1.4	1.6	1.5	1.5	1.7	1.5	1.5	1.5	1.5
Fe^{2+}	3.0	2.8	2.8	2.8	2.6	2.8	2.8	2.7	2.8
[2]Fe^{3+}	0.3	0.3	0.3	0.3	0.3	0.3	0.3	0.3	0.3
Mg	1.1	1.0	1.1	1.2	1.0	1.1	1.1	1.2	1.1
Total	9.8	9.7	9.7	9.8	9.6	9.7	9.7	9.7	9.7
Fe/(Fe + Mg)	0.7	0.8	0.7	0.7	0.7	0.7	0.7	0.7	0.7

Chemical formulae normalized to an anion basis of $O_{10}(OH)_8$.
[1] Each value is an average of 3 analyses of an individual grain.
[2] 10% of total Fe is assumed to be Fe^{3+} (see, McDowell and Elders, 1980).

1983; Lee, 1984), mixed layering of chlorite and 1:1 phyllosilicates has not been recognized as frequently, mainly because of the difficulties encountered in identifying such assemblages with XRD. Interstratification of 7- and 14-Å layers, however, can easily be identified by TEM techniques directly from lattice fringe images.

Chlorites from the 2450- and 5500-m samples commonly consist of 14-Å layers interstratified with 7-Å layers (Figures 2 and 3). Rarely, chlorite grains have abundant 7-Å layers randomly mixed with 14-Å layers (Figure 6). The packets of interstratified 7-Å layers vary from one to six layers with no apparent ordering of the 14-Å layers (Figure 6). Electron diffraction patterns of random interstratification of 7- and 14-Å layers are characterized by weak $00l$ reflections, with l = odd and diffuse streaking parallel to c*. Dean (1983) observed, from XRD patterns, a broadening and weakening of
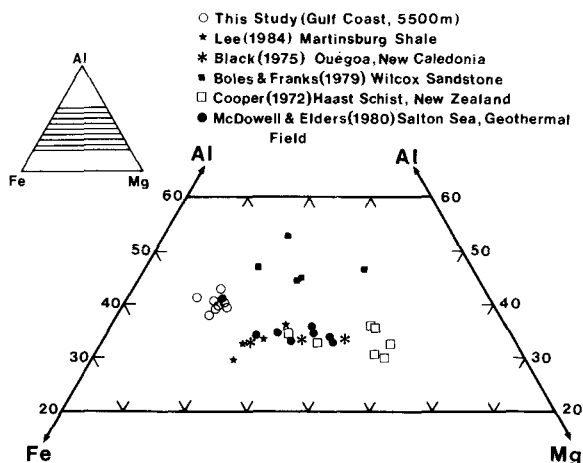

Figure 5. Composition of chlorite from the 5500-m depth of Gulf Coast plotted on an Al-Fe-Mg diagram. Other chlorites from diagenetic and metamorphic environments are plotted for comparison.
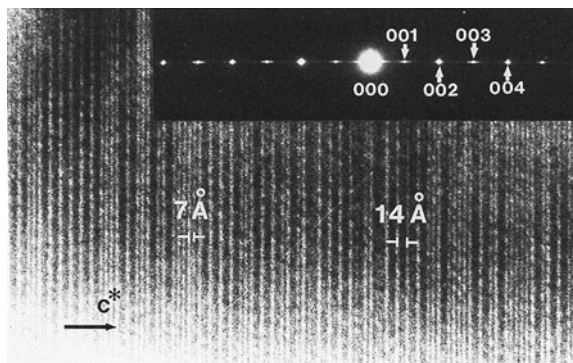

Figure 6. Lattice fringe image and electron diffraction pattern of 7–14-Å mixed-layer chlorite. 7-Å layers are randomly interlayered within chlorite with varying thickness of units.

$00l$ reflections with l = odd from chlorite that coated sand grains from Cold Lake, Alberta, and proposed that these line profiles were due to interstratification of 7- and 14-Å layers. Our observations thus support his hypothesis.

Because the packets of 7-Å layers were not large enough to provide single-phase analytical data, even by AEM techniques, chemical data were obtained in an indirect manner. AEM analytical data were obtained on a region of pure chlorite (Table 1) and on a region containing abundant 7-Å layers within 14-Å layers to get comparative data for the 7-Å layers (Table 2). If the 7-Å phase had been kaolinite, the chemical composition of the regions containing both 7- and 14-Å layers (Table 2) should have shown much higher Al and Si contents than pure chlorite (Table 1). Both regions showed, however, almost the same values for Al and Si; therefore, the 7-Å phase is likely an Fe-rich, aluminous trioctahedral phase, as are the 14-Å layers. One minor difference between the coexisting 14-Å and 7-Å phases is that the 7-Å phase is apparently slightly richer in Fe than the 14-Å layers. To a first approximation, however, the 7- and 14-Å layers have the same composition and are therefore polymorphs, *sensu stricto*. Thus, the 7-Å layers are an Fe-rich, aluminous trioctahedral phase similar to berthierine as defined by Bailey (1980) and Brindley (1982). The nomenclature for such 7-Å phases, however, is not well defined, and the proper names used for specific phases are subject to question (S. W. Bailey, Department of Geology and Geophysics, University of Wisconsin, Madison, Wisconsin, personal communication, 1984).

DISCUSSION AND CONCLUSIONS

Chlorite formation in burial diagenesis

Many investigators have suggested that kaolinite is a major source of Al and Si for chlorite during burial diagenesis because chlorite generally increases in abundance over the same depth interval in which kaolinite decreases in abundance (Muffler and White, 1969;

Table 2. Analytical electron microscopic analyses of 7-Å/14-Å mixed-layer chlorite from the 5500-m sample.

Elements	[1]1	2	3	Average
Si	2.7	2.7	2.7	2.7
Al(IV)	1.3	1.3	1.3	1.3
Al(VI)	1.3	1.6	1.4	1.4
Fe^{2+}	3.3	3.0	3.2	3.2
[2]Fe^{3+}	0.4	0.3	0.4	0.4
Mg	0.8	0.8	0.9	0.8
Total	9.8	9.7	9.9	9.8
Fe/(Fe + Mg)	0.8	0.8	0.8	0.8

Chemical formulae normalized to an anion basis of $O_{10}(OH)_8$.

[1] Each value is an average of 3 analyses of an individual grain.

[2] 10% of total Fe is assumed to be Fe^{3+} (see, McDowell and Elders, 1980).

Perry and Hower, 1970; Heling, 1978; Boles and Franks, 1979). Boles and Franks (1979) suggested that the high aluminum content of the chlorite from the Wilcox sandstone was inherited from kaolinite and proposed a reaction of kaolinite to chlorite with Fe and Mg being supplied by smectite during its transition to illite. Hower et al. (1976), however, showed no systematic decrease in kaolinite over the depth interval where chlorite formed. All incipient-stage chlorites from the 2450-m samples (Figures 1 and 2) occur exclusively as part of and within grains of I/S. This distribution strongly implies that the formation of chlorite was closely related to I/S rather than to kaolinite.

On the other hand, Dunoyer de Segonzac (1970) suggested that the diagenetic formation of chlorite is preceded by an intermediate stage of corrensite or mixed-layer chlorite/smectite formation through the fixation of Mg in interlayer sites of smectite. Several experimental studies appear to have documented the transformation of smectite to a chlorite-like structure by fixation of Mg in a smectite structure (Caillère and Henin, 1949; Slaughter and Milne, 1960; Besson et al., 1966), but the products displayed characteristics which were intermediate between those of vermiculite and chlorite. No experimental data have been reported that show the direct transformation of smectite to an ideal chlorite structure.

Many TEM studies have described the local transformation of biotite to chlorite (e.g., Iijima and Zhu, 1982; Olives et al., 1983; Veblen, 1983; Veblen and Ferry, 1983), but none have documented the transformation of a dioctahedral 2:1 sheet structure to a trioctahedral chlorite structure. The direct solid-state transformation of dioctahedral smectite to trioctahedral chlorite is not likely; the necessary insertion of brucite-like layers between dioctahedral smectite layers only accounts for the topology of the structure of a dioctahedral chlorite (Eberl, 1978). The compositions of the octahedral and tetrahedral layers of smectite must change radically in order to achieve the composition of a trioctahedral chlorite. Another difficulty is that 7-Å berthierine interstratified with chlorite as revealed by our TEM observations requires that the dioctahedral 2:1 layer structure of smectite locally transforms to both a trioctahedral 14-Å structure and a trioctahedral 7-Å structure simultaneously. This requires that the tetrahedral and octahedral layers be disrupted to convert the dioctahedral smectite to the trioctahedral chlorite.

Hower et al. (1976), however, proposed a general reaction which occurs during burial diagenesis of shale: smectite + K-feldspar + mica = illite + chlorite + quartz. In clay separates consisting almost entirely of I/S, they found a large increase in K_2O and Al_2O_3 and a decrease in SiO_2, Fe_2O_3, and MgO with increasing depth. They attributed the chemical change to a smectite to illite transformation, smectite + Al^{3+} + K^+ = illite + Si^{4+}. They also suggested that the actual reaction is much more complex and that Fe and Mg are lost from smectite layers. Hower et al. (1976) proposed that Fe and Mg released from smectite can be a major source of the trioctahedral components of chlorite. On the basis of direct AEM data from smectite and transformed illite, Ahn et al. (1983) and Ahn and Peacor (1984) reported a substantial decrease in Fe and Mg during the transformation of smectite to illite.

The present AEM data (Table 1) show that the average chemical formula of chlorite from the Gulf Coast in the 5500-m sample is $Fe_{3.1}Mg_{1.1}Al_{2.7}Si_{2.8}O_{10}(OH)_8$, indicating that the chlorite is highly enriched in Fe relative to Mg with an average Fe/(Fe + Mg) value of approximately 0.7. In addition, and most importantly, the chemical data from Hower et al. (1976) show a greater decrease in Fe_2O_3 than in MgO in fractionated clays (mostly I/S) with increasing depth and illite proportion in I/S. This chemical change suggests that smectite layers lose more Fe than Mg during their conversion to illite. The high value of Fe/(Fe + Mg) in diagenetic chlorite can therefore be explained by such a preferential loss of Fe from smectite and strongly implies that Fe and Mg from smectite are the major source of those elements for chlorite formation. As noted above, the texture of the chlorite in the samples also support this relation in that chlorite occurs exclusively within I/S at incipient stages of formation; these chlorite layers are intergrown parallel to and are semicoherent with layers of surrounding I/S.

Furthermore, the XRD data of Hower et al. (1976) demonstrate that the depth beyond which the relative amount of chlorite remains constant (3700 m), coincides with the depth where the conversion of smectite to illite ceases. They observed that beyond this depth the proportion of illite (80%) in I/S remained constant. The coincidence of the depths beyond which illite and chlorite remain constant in abundance is compatible with the relation that chlorite cannot form below that

depth as there is no longer a supply of Fe and Mg. Thus, the diagenetic chlorite in the Gulf Coast shale appears to have formed by a process which involved considerable diffusion and recrystallization by utilizing Fe and Mg released from smectite rather than by direct solid-state transformation from smectite or kaolinite. The chlorite was a direct byproduct of the smectite to illite transformation. The Si may have been provided by smectite in that Si was released along with Fe and Mg during transformation of the smectite to illite or it could have been supplied by the decomposition of other detrital silicate minerals (e.g., K-feldspar and/or mica). K-feldspar and detrital micas were observed to decrease and finally to disappear with increasing depth (Perry and Hower, 1970; Hower *et al.,* 1976) in the same depth interval where illite and chlorite increased in abundance.

7-Å layers within chlorite

From clinochlore synthesis data Yoder (1952) suggested that "7-Å chlorite" is a low-temperature polymorph of "14-Å chlorite." Subsequently, many investigators observed that a 7-Å phase always preceded the formation of chlorite in studies of synthetic chlorites (Nelson and Roy, 1958; Gillery, 1959; Turnock, 1959, 1960; Fawcett and Yoder, 1966; Velde, 1973; James *et al.,* 1976; Cho and Fawcett, 1982). Although such 7-Å phases have only rarely been reported from pelitic rocks (Frey, 1970, 1978; Lee and Peacor, 1983), 7-Å layers associated with chlorite have been reported from various shallow environments, implying a polymorphic transition from the 7-Å to the 14-Å phase (Brindley and Gillery, 1954; Millot, 1964; Iijima and Matsumoto, 1982). Frey (1970, 1978) stated that "7-Å chlorite" should be more common in pelitic rocks than reported, but the apparent rareness of phases such as berthierine is due, in part, to the difficulty in identifying it by XRD techniques because of overlap of its 00*l* peaks with those of chlorite. The lowest temperature for the transition of a 7-Å phase to chlorite was reported by Nelson and Roy (1958) to be 450°–500°C, but Velde (1973) observed that the 7-Å to 14-Å transition occurred below 400°C in Mg chlorite. Turnock (1960) and James *et al.* (1976) observed that the temperature of transformation in iron chlorite was much higher than that of Mg chlorite and was as high as 525°C; however, no reliable evidence has been reported that a 7-Å phase has a true stability field with respect to chlorite. Rather, the data are consistent with the interpretation that the 7-Å phase forms metastably at low temperature as a precursor to the 14-Å phase.

The berthierine interstratified within chlorite showed no significant difference in frequency of occurrence between the 2450-m and 5500-m samples. The temperatures corresponding to the 2450-m and 5500-m depths are 70°C and 165°C, respectively (Hower *et al.,* 1976). Although there is almost a 100°C difference between these two depths, no significant change in abundance of berthierine has been noted. Some chlorite from the 2450-m sample contains no berthierine (Figure 1), and no discrete berthierine packets free of chlorite have been observed. This type of occurrence of the 7-Å phase implies that all of the chlorite was not necessarily preceded by such a 7-Å phase even at low temperatures, contrary to the results of some experimental studies.

Finally, because the 7-Å layers and chlorite have nearly the same compositions, they are polymorphically related; because they coexist over a range of temperature, they must therefore coexist in a non-equilibrium relation, i.e., the 7-Å layers are metastable relative to the 14-Å layers. The formation of 7-Å layers would be aided by relatively rapid crystallization at low temperatures where kinetic effects are favorable for such relations. Yau *et al.* (1984) also observed 7-Å layers interlayered with chlorite only at shallow depth samples of the Salton Sea geothermal field based on TEM studies. With extreme burial diagenesis or very low grade metamorphism, the 7-Å layers presumably become increasingly scarce (see, e.g., Lee, 1984). Trioctahedral 7-Å layers should therefore be more common in a burial diagenetic environment and in the shallower depths. The rarity of the trioctahedral 7-Å phase as described in the literature may simply be due to difficulties in identifying it by XRD methods. Because it occurs in small amounts and it is usually interstratified with chlorite, its presence may be detected only using TEM methods.

ACKNOWLEDGMENTS

REFERENCES

Ahn, J. H., Lee, J. H., and Peacor, D. R. (1983) Mineralogical and textural transition in phyllosilicates during burial diagenesis of Gulf Coast shales: *Geol. Soc. Amer. Abstr. Progr.* **15,** p. 512 (abstract).

Ahn, J. H. and Peacor, D. R. (1984) The smectite to illite transformation in Gulf Coast argillaceous sediments based on microstructure by TEM/AEM: in *Program with Abstracts, 21st Annual Meeting of The Clay Minerals Society, Baton Rouge, Louisiana, 1984,* p. 22 (abstract).

Allard, L. F., Blake, D. F., Newberry, N. G., Bigelow, W. C., and Peacor, D. R. (1980) Microanalysis of geological materials in an analytical electron microscope: elimination of spectral contamination: *EOS Trans. Amer. Geophys. Union* **61,** p. 398 (abstract).

April, R. H. (1981) Trioctahedral smectite and interstrati-

fied chlorite/smectite in Jurassic strata of the Connecticut Valley: *Clays & Clay Minerals* **29**, 31–39.

Bailey, S. W. (1980) Structures of layer silicates: in *Crystal Structures of Clay Minerals and Their X-ray Identification,* G. W. Brindley and G. Brown, eds., Mineralogical Society, London, 1–123.

Besson, H., Caillère, S., and Henin, M. S. (1966) Comportement d'une montmorillonite en présene d'une solution magnésienne: formation d'une pseudochlorite stable: *Bull. Groupe Franç. Argiles* **18**, 51–53.

Black, P. M. (1975) Mineralogy of New Caledonia metamorphic rocks: IV. Sheet silicates from the Ouégoa District: *Contrib. Mineral. Petrol.* **49**, 269–284.

Blake, D. F., Allard, L. F., Peacor, D. R., and Bigelow, W. C. (1980) "Ultraclean" X-ray spectra in the JEOL JEM-100CX: in *Proc. 38th Ann. Meeting, Electron Microsc. Soc. Amer., San Francisco, California, 1980,* G. W. Bailey, ed., Claitor's Publishing Division, Baton Rouge, Louisiana, 136–137.

Boles, J. R. and Franks, S. G. (1979) Clay diagenesis in Wilcox sandstones of southwest Texas: implications of smectite diagenesis on sandstone cementation: *J. Sed. Petrol.* **49**, 55–70.

Brindley, G. W. (1982) Chemical compositions of berthierines—a review: *Clays & Clay Minerals* **30**, 153–155.

Brindley, G. W. and Gillery, F. H. (1954) A mixed-layer kaolin-chlorite structure: in *Clays and Clay Minerals, Proc. 2nd Natl. Conf., Columbia, Missouri, 1953,* A. Swineford and N. Plummer, eds., *Natl. Acad. Sci. Natl. Res. Counc. Publ.* **327**, Washington, D.C., 349–353.

Brown, B. E. and Bailey, S. W. (1962) Chlorite polytypism: I. Regular and semi-random one-layer structures: *Amer. Mineral.* **47**, 819–850.

Caillère, S. and Henin, S. (1949) Experimental formation of chlorites from montmorillonite: *Mineral. Mag.* **28**, 612–620.

Cho, M. and Fawcett, J. J. (1982) Mechanism and kinetics of the reaction, clinochlore = forsterite + cordierite + spinel + vapor: *AGU East Coast Meeting, EOS* **63**, p. 465 (abstract).

Cliff, G. and Lorimer, G. W. (1975) The quantitative analysis of thin specimens: *J. Microsc.* **103**, 203–207.

Cooper, A. F. (1972) Progressive metamorphism of metabasic rocks from the Haast schist group of southern New Zealand: *J. Petrol.* **13**, 457–492.

Dean, R. S. (1983) Authigenic trioctahedral clay minerals coating Clearwater Formation sand grains at Cold Lake, Alberta, Canada: in *Programs and Abstracts, 20th Annual Meeting of The Clay Minerals Society, Buffalo, New York, 1983,* p. 79 (abstract).

Dunoyer de Segonzac, G. (1970) The transformation of clay minerals during diagenesis and low-grade metamorphism: a review: *Sedimentology* **15**, 281–346.

Eberl, D. (1978) Reaction series for dioctahedral smectite: *Clays & Clay Minerals* **26**, 327–340.

Fawcett, J. J. and Yoder, H. S., Jr. (1966) Phase relationships of chlorites in the system MgO-Al$_2$O$_3$-SiO$_2$-H$_2$O: *Amer. Mineral.* **51**, 353–380.

Foster, M. D. (1962) Interpretation of composition and a classification of the chlorites: *U.S. Geol. Surv. Prof. Pap.* 414-A, 1–33.

Frey, M. (1970) The step from diagenesis to metamorphism in pelitic rocks during Alpine orogenesis: *Sedimentology* **15**, 261–279.

Frey, M. (1978) Progressive low-grade metamorphism of a black shale formation, central Swiss Alps, with special reference to pyrophyllite and margarite bearing assemblage: *J. Petrol.* **19**, 95–135.

Gillery, F. H. (1959) The X-ray study of synthetic Mg-Al serpentines and chlorites: *Amer. Mineral.* **44**, 143–152.

Hayes, J. B. (1970) Polytypism of chlorite in sedimentary rocks: *Clays & Clay Minerals* **18**, 285–306.

Heling, D. (1978) Diagenesis of illite in argillaceous sediments of the Rhinegraben: *Clay Miner.* **13**, 211–220.

Hower, J., Eslinger, E. V., Hower, M. E., and Perry, E. A. (1976) Mechanism of burial metamorphism of argillaceous sediment: 1. Mineralogical and chemical evidence: *Geol. Soc. Amer. Bull.* **87**, 725–737.

Iijima, A. and Matsumoto, R. (1982) Berthierine and chamosite in coal measures of Japan: *Clays & Clay Minerals* **30**, 264–274.

Iijima, S. and Buseck, P. R. (1978) Experimental study of disordered mica structure by high-resolution electron microscopy: *Acta Crystallogr.* **A34**, 709–719.

Iijima, S. and Zhu, J. (1982) Electron microscopy of a muscovite-biotite interface: *Amer. Mineral.* **67**, 1195–1205.

James, R. S., Turnock, A. C., and Fawcett, J. J. (1976) The stability and phase relations of iron chlorite below 8.5 kb P$_{H_2O}$: *Contrib. Mineral. Petrol.* **56**, 1–25.

Lee, J. H. (1984) Mineralogical studies of phyllosilicates in a slaty cleavage development in the Martinsburg Formation near Lehigh Gap, Pennsylvania: TEM-AEM study: Ph.D. thesis, Univ. Michigan, Ann Arbor, Michigan, 221 pp.

Lee, J. H. and Peacor, D. R. (1983) Interlayer transitions in phyllosilicates of Martinsburg shale: *Nature* **303**, 608–609.

Maresch, W. V., Massone, H.-J., and Czank, M. (1983) An ordered 1–1 chlorite/biotite mixed-layer mineral as an alteration of chlorite: *Fortschr. Mineral.* **61**, 139–141.

McDowell, S. D. and Elders, W. A. (1980) Authigenic layer silicate minerals in borehole Elmore 1, Salton Sea Geothermal Field, California, U.S.A.: *Contrib. Mineral. Petrol.* **74**, 293–310.

Millot, G. (1964) *Géologie des Argiles:* Masson et Cie, Paris, 500 pp.

Muffler, L. J. P. and White, D. E. (1969) Active metamorphism of upper Cenozoic sediments in the Salton Sea geothermal field and the Salton Trough, southeastern California: *Geol. Soc. Amer. Bull.* **80**, 157–182.

Nelson, B. W. and Roy, R. (1958) Synthesis of chlorites and their structural and chemical constitution: *Amer. Mineral.* **43**, 707–725.

Olives, B. J., Amouric, M., de Fouquet, C., and Baronnet, A. (1983) Interlayering and interlayer slip in biotite as seen by HRTEM: *Amer. Mineral.* **68**, 754–758.

Perry, E. and Hower, J. (1970) Burial diagenesis in Gulf Coast pelitic sediments: *Clays & Clay Minerals* **18**, 165–177.

Schreyer, W., Medenbach, O., Abraham, K., Begert, W., and Müller, W. F. (1982) Kulkeite, a new metamorphic phyllosilicate mineral: ordered 1:1 chlorite/talc mixed layer: *Contrib. Mineral. Petrol.* **80**, 103–109.

Slaughter, M. and Milne, I. H. (1960) The formation of chlorite-like structures from montmorillonite: in *Clays and Clay Minerals, Proc. 7th Natl. Conf., Washington, D.C., 1958,* A. Swineford, ed., Pergamon Press, New York, 114–125.

Turnock, A. C. (1959) Stability range of iron chlorite: *Geol. Soc. Amer. Bull.* **70**, 1690–1691.

Turnock, A. C. (1960) The stability of iron chlorites: *Carnegie Inst. Wash. Year Book* **59**, 98–103.

Veblen, D. R. (1983) Microstructures and mixed layering in intergrown wonesite, chlorite, talc, biotite and kaolinite: *Amer. Mineral.* **68**, 566–580.

Veblen, D. R. and Ferry, J. M. (1983) A TEM study of biotite-chlorite reaction and comparison with petrologic observations: *Amer. Mineral.* **68**, 1160–1168.

Velde, B. (1973) Phase equilibria studies in the system MgO-Al$_2$O$_3$-SiO$_2$-H$_2$O: chlorite and associated minerals: *Mineral. Mag.* **39**, 297–312.

Velde, B. (1977) *Clays and Clay Minerals in Natural and Synthetic Systems:* Elsevier, Amsterdam, 218 pp.

Velde, B., Raoult, J. F., and Leikine, M. (1974) Metamorphosed berthierine pellets in Mid-Cretaceous rocks from northeastern Algeria: *J. Sed. Petrol.* **44,** 1275–1280.

Weaver, C. E. and Beck, K. C. (1971) Clay-water diagenesis during burial: how mud becomes gneiss: *Geol. Soc. Amer. Spec. Pap.* **134,** 96 pp.

Yau, L. Y. C., Peacor, D. R., and McDowell, S. D. (1984) TEM/AEM study of chlorite diagenesis in well I.I.D. No. 2 in Salton Sea geothermal field, California: in *Program with Abstracts, 21st Annual Meeting of the Clay Minerals Society, Baton Rouge, Louisiana, 1984,* p. 120 (abstract).

Yoder, H. S. (1952) The MgO-Al$_2$O$_3$-SiO$_2$-H$_2$O system and the related metamorphic facies: *Amer. J. Sci. Bowen Vol.,* 569–629.